MedChemComm

RSC Publishing

CONCISE ARTICLE

View Article Online
View Journal | View Issue

Published on 22 October 2013. Downloaded by University of California - Irvine on 31/10/2014 12:28:36.

Cite this: *Med. Chem. Commun.*, 2013, **4**, 1619

Ketorolac beats ketoprofen: lower photodecarboxylation, photohemolysis and phototoxicity†

Christopher D. McTiernan,[a] Chiara Fasciani,[a] Maria González-Béjar,[b] Daniel Roca-Sanjuán,[b] Emilio I. Alarcon*[a] and Jose Carlos Netto-Ferreira*[ac]

Received 10th September 2013
Accepted 16th October 2013

DOI: 10.1039/c3md00258f

www.rsc.org/medchemcomm

Ketorolac shows reduced photohemolytic activity and low phototoxicity against human skin fibroblasts when compared to ketoprofen. The low decarboxylation quantum yield together with the efficient non-radiative deactivation of the triplet and singlet excited states of ketorolac are believed to be responsible for this behaviour.

The presence of a benzophenone-like moiety in many pharmaceutical compounds, including non-steroidal anti-inflamatory drugs (NSAID), has been related to their phototoxicity due to the generation of reactive intermediates upon drug photodecomposition.[1–3] For example, the main pathway for ketoprofen photodegradation upon UVA light exposure, at physiological pH, is photodecarboxylation.[1] Such decarboxylation has been related to the generation of free radicals and the formation of hemolytic holes.[4] Further, formation of methemoglobin free radicals has been also reported upon UVA exposure of erythrocyte suspensions containing ketoprofen.[5] Thus, both processes are believed to play key roles in the photohemolysis of human erythrocytes mediated by ketoprofen. Ketorolac, on the other hand, is a powerful analgesic commonly administrated after dental procedures, including root canals and tooth extractions, as well as in eye-drops for glaucoma pain control.[6] Although this NSAID is commonly prescribed and shares a benzoyl group with ketoprofen, see Scheme 1, there have been documented studies on its toxicity in humans, see for example ref. 7 & 8, and little is known of its photophysics and photochemistry. The following presents our findings on the photohemolysis, cell phototoxicity, photophysics, and photochemistry for ketorolac.

Interestingly, when red blood cell suspensions ($\approx 3.3 \times 10^6$ cells per ml) containing 10, 30, or 60 μM ketoprofen, ketorolac, or their corresponding decarboxylated photoproducts are exposed to UVA light for 15 min varying degrees of photohemolytic activity are observed (see Fig. 1). For example, while ketoprofen shows photohemolytic activity in the whole range of concentrations, ketorolac displays only a 20% hemolysis at its highest concentration. Noticeably, the ketoprofen photoproduct showed a dose dependent behaviour in its hemolytic activity. In contrast, the ketorolac photoproduct did not show any toxicity even at the highest concentration tested.

In addition, phototoxicity experiments carried out on skin fibroblasts cultures revealed non-toxicity of ketorolac and relative phototoxicities for the other compounds as follows: ketoprofen photoproduct > ketoprofen ≈ ketorolac photoproduct, see Fig. 2. Although a direct comparison between the hemolysis and fibroblasts toxicity data is not possible due to differences in uptake and metabolism between the two cell lines, our cumulative data suggests that ketorolac is not toxic upon UVA exposure. Differences in the decarboxylation quantum yield between ketorolac and ketoprofen are likely responsible for the differences in toxicity data.

In fact a decarboxylation quantum yield as low as 8.0×10^{-5} was measured for ketorolac (Fig. 3). This value is almost five orders of magnitude smaller than that reported for ketoprofen.[1] However, the reason for the difference in the photoreactivity of these two compounds is not yet clear. Therefore, further photophysical and photochemical characterization of ketorolac was carried out.

The absorption spectrum of ketorolac presents a high intensity band around 300 nm (Fig. S1†). According to theoretical CASPT2 computations (see ESI; Fig. S2–S4 and Tables S1–S4†), the lowest-energy band can be ascribed to an excited state featuring a transfer of electron density from the pyrrole moiety to the keto group (see Fig. 4).

[a]*Department of Chemistry and Centre for Catalysis Research and Innovation, University of Ottawa, 10 Marie Curie, Ottawa K1N 6N5, Canada. E-mail: emilio@photo.chem.uottawa.ca; josecarlos@photo.chem.uottawa.ca*

[b]*Instituto de Ciencia Molecular, Universidad de Valencia, C/Catedrático José Beltrán, 2, Paterna, 46980, Valencia, Spain*

[c]*Departamento de Química, Universidade Federal Rural do Rio de Janeiro, Seropédica, 23851-970, Rio de Janeiro, Brazil*

† Electronic supplementary information (ESI) available: Materials, syntheses and characterization, theoretical methods and analyses, phototoxicity experiments carried out on skin fibroblasts cultures, ketorolac UV-Visible spectra in acetonitrile or in phosphate buffer, 1/kobs at 620 nm as function of 1-methyl naphthalene, singlet oxygen phosphorescence, phosphorescence. See DOI: 10.1039/c3md00258f

Published on 22 October 2013. Downloaded by University of California - Irvine on 31/10/2014 12:28:36.

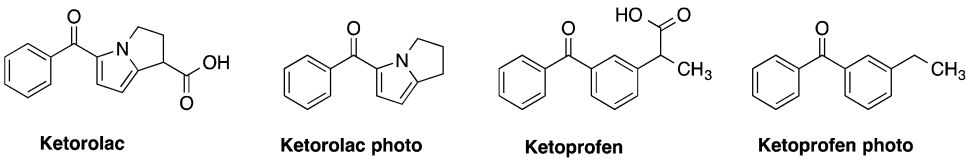

Scheme 1 Chemical structures of Ketorolac, Ketoprofen, and their corresponding decarboxylated photoproducts identified as "photo".

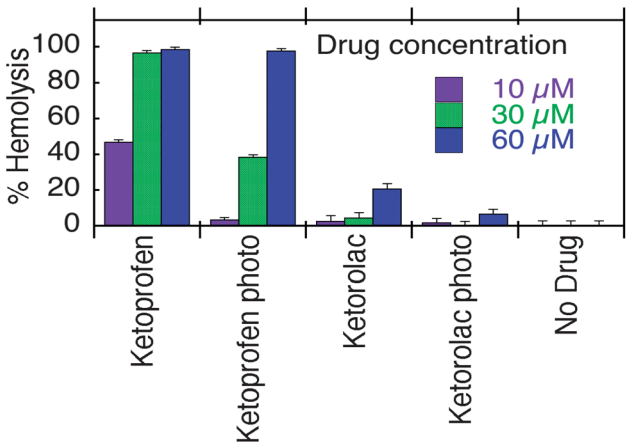

Fig. 1 Photohemolytic activity for ketorolac, ketoprofen and their respective decarboxylation products (Scheme 1).

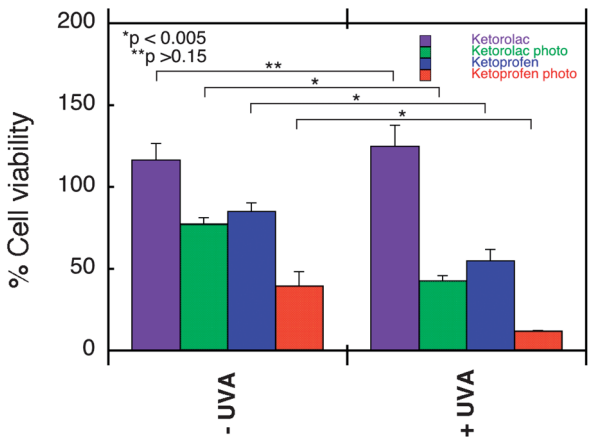

Fig. 2 Phototoxicity experiments carried out on skin fibroblasts. Results obtained using an MTS viability assay. The parental drugs and their corresponding decarboxylated photoproduct were added as 1 mM solutions in FCS supplemented DMEM containing 10% DMSO. See SI for complete details (plate P6).

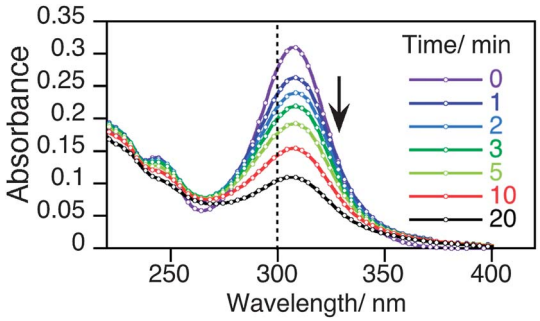

Fig. 3 Time evolution profile for the photodecomposition of 10 μM ketorolac to afford its corresponding decarboxylated photoproduct, see experimental. All measurements were carried out in nitrogen-saturated solutions at RT.

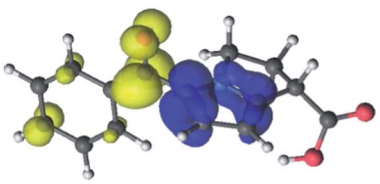

Fig. 4 CASSCF electron-density difference between the ground and the lowest-lying excited singlet states at the CASSCF optimized gas-phase structure of the later. Regions with an excess and deficiency of electron density are in yellow and blue, respectively.

A red-shift (14 nm) is observed in aqueous solutions proving the polarizability of the singlet state (Fig. S1†). This agrees with its charge transfer nature and the theoretical analysis of solvent effects (see ESI†). Moreover, no fluorescence emission was detected for this compound in acetonitrile or buffer solution.

Upon laser excitation (266 nm) of deareated ketorolac in acetonitrile, the presence of two intermediate species was observed (Fig. 5). The first one has a lifetime of 2.5 μs with absorption maxima at 350 and 620 nm, and is readily quenched by oxygen (2.0×10^9 M^{-1} s^{-1}) (Table 1). Quenching experiments carried out using 1-methyl naphthalene rendered a rate constant of 1.5×10^9 M^{-1} s^{-1}, fully compatible with an energy transfer mechanism[9,10] (Fig. S5).† Thus, the 620 nm transient species was assigned to the ketorolac triplet with a quantum yield of only 0.18. Also a singlet oxygen quantum yield of 0.06 was obtained when ketorolac was employed as sensitizer, corresponding to a singlet oxygen efficiency of ≈0.33 (Fig. S6†). This value is in full agreement with those observed for singlet oxygen efficiency of other ^{3}n,π* systems such as acetophenone.[11] Further, low temperature phosphorescence measurements indicate that the ketorolac triplet state shows a ^{3}n,π* character with 2.73 eV energy; Fig. S7.† A similar conclusion is drawn from the bimolecular rate constants measured using several triplet quencher molecules (Table 1) and CASPT2 results (even though the presence of a triplet ^{3}π,π* state is also estimated at close energies and might contribute to the band at higher wavelengths, Tables S5–S6†).

Interestingly, activation energies for the ketorolac triplet state as low as 1.0 and 1.5 kcal mol^{-1} for acetonitrile and PBS buffer, respectively, were obtained from Arrhenius plots (Fig. S8†), with pre-exponential factors in the order of ≈10^8 s^{-1}.

This journal is © The Royal Society of Chemistry 2013

Published on 22 October 2013. Downloaded by University of California - Irvine on 31/10/2014 12:28:36.

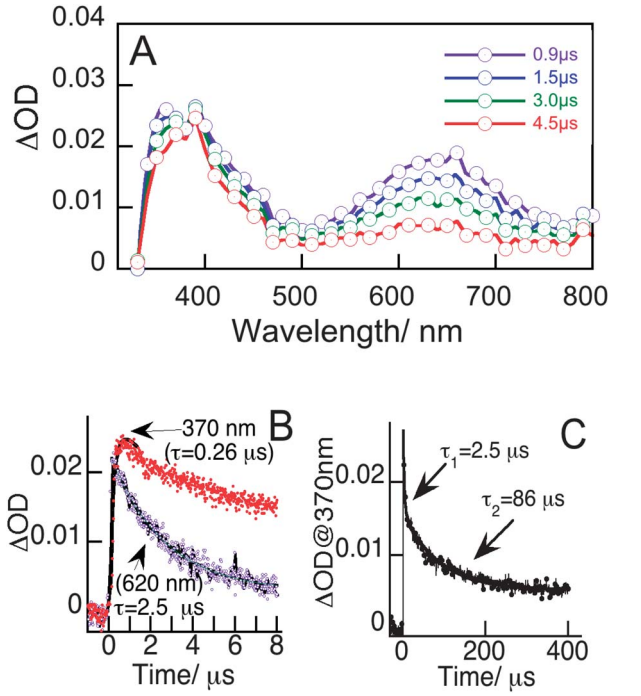

Fig. 5 (A) Ketorolac (50 μM) transient absorption spectra at different times after 266 nm laser excitation. (B) 370 nm and 620 nm decay profiles at short time scale. (C) Inset: 370 nm transient time profile.

Table 1 Bimolecular quenching rate constants for Ketorolac triplet state with different quenchers

Quencher	k_q (M^{-1} s^{-1}) × 10^6
Oxygen	2000 ± 100
1,4-Cyclohexadiene	4.80 ± 0.10
2-Propanol[a]	0.47 ± 0.01
2-Propanol[b]	0.65 ± 0.05
L-Tryptophan methyl ester	1500 ± 100
L-Tyrosine methyl ester	3000 ± 100
2′-Deoxyguanosine	270 ± 10

[a] Measured in acetonitrile. [b] Measured in dichloromethane.

Thus, the presence of an adiabatic deactivation route where spin multiplicity is conserved seems to be the pathway responsible for triplet deactivation.

The second intermediate observed upon laser excitation (Fig. 5B and C) showed a rise time of ≈260 ns with a strong absorbance at 370 nm. This species has a lifetime of ≈86 μs and is readily quenched by oxygen at a diffusion-controlled rate constant of 1×10^{10} M^{-1} s^{-1}. A similar intermediate was detected for ketorolac ester and 2-benzoylpyrrole (Fig. S9 and S10†), indicating that the origin of this intermediate is directly related to the benzoylpyrrole moiety. Further, although time-resolved experiments for ketorolac in buffer solutions also led to similar intermediates, the triplet lifetime was only 0.2 μs. Note that under these conditions HCl addition produced a 60% quenching of the long-lived transient (data not shown). This result suggests the formation of an *enolate*-like intermediate for ketorolac as the most likely responsible for this long-lived intermediate. Theoretical analyses point out to the population of the antibonding π* orbital of the ketone group of ketorolac in the lowest-lying singlet and triplet excited states. As a consequence, the relaxation of the ^{3}n,π* state to the corresponding equilibrium structure results in an enlargement of the CO bond distance from 1.22 to 1.36 Å (Table S6†), thus increasing the basicity of the *keto* group as explained elsewhere.[12,13]

The formation of an *enol*-like intermediate is in good agreement with the reported oxidation products in literature.[14,15] The reason why the *enol* intermediate for ketorolac appears in time scales where the triplet is still decaying (Fig. 5B) is probably due to the presence of mixing states for the ketorolac triplet as revealed from computational calculations (Tables S5 and S6†). In this case only the short-lived ^{3}n,π* would lead to the *enol* formation.

Finally, we have addressed how the ketorolac triplet-excited state is competitively deactivated but have not discussed its lack of fluorescence as well as its low triplet quantum yield. From our modest computational approach, we expect that the corresponding radiationless decay mechanism will be initially driven by the intra-molecular charge transfer, ICT, nature of the singlet-excited state (see Fig. 4). An enlargement of the CO bond distance and a rearrangement of the relative orientation between the benzoyl and pyrrole moieties might bring the system to an internal conversion process, as it happens in other molecules such as the cytosine DNA base.[16,17] More advanced computational strategies shall, however, be required in future studies to accurately determine the deactivation channel of the bright state of ketorolac.

Conclusions

In summary, our findings show a lack of fluorescence and low triplet quantum yield and decarboxylation efficiency for ketorolac. The formation of an *enol* intermediate is proposed to be responsible for the formation of a long-lived intermediate from the triplet-excited state and an ICT excited state may be expected to initiate the radiationless decay of the molecule on the singlet manifold. Such a complex photophysical pathway helps explain the low photohemolytic activity and reduced phototoxicity of ketorolac. These results open a new paradigm on the, until now, well-known photophysical behavior of NSAIDs.

Acknowledgements

We gratefully acknowledge NSERC and The Spanish Ministry of Economy and Competitiveness (CTQ2011-27758, CTQ2010-14892; M.G.B. Juan de la Cierva contract) for support of this research. J.C.N.-F. thanks the University of Ottawa for a Visiting Professor fellowship. C.F. gratefully acknowledges NSERC and the Vanier CGS program. Lastly, the authors would like to thank Michel Grenier for his help in the time resolved measurements and Professor Juan C. Scaiano for helpful discussions and comments on the article.

Published on 22 October 2013. Downloaded by University of California - Irvine on 31/10/2014 12:28:36.

Notes and references

1 G. Cosa, M. Lukeman and J. C. Scaiano, *Acc. Chem. Res.*, 2009, **42**, 599–607.
2 G. Cosa, L. Llauger, J. C. Scaiano and M. A. Miranda, *Org. Lett.*, 2002, **4**, 3083–3085.
3 L. Llauger, M. A. Miranda, G. Cosa and J. C. Scaiano, *J. Org. Chem.*, 2004, **69**, 7066–7071.
4 L. L. Costanzo, G. D. Guidi, G. Condorelli, A. Cambria and M. Fama, *Photochem. Photobiol.*, 1989, **50**, 359–365.
5 Y.-Y. He, D. C. Ramirez, C. D. Detweiler, R. P. Mason and C. F. Chignell, *Photochem. Photobiol.*, 2003, **77**, 585–591.
6 D. A. Handley, P. Cervoni, J. E. McCray and J. R. McCullough, *J. Clin. Pharmacol.*, 1998, **38**, 25–35.
7 L. A. Boras-Uber and N. C. Brackett Jr, *Am. J. Med.*, 1992, **92**, 450–452.
8 M. L. Randi, T. Tison, G. Luzzatto and A. Girolami, *BMJ.*, 1993, **306**, 186.
9 N. J. Turro, V. Ramamurthy and J. C. Scaiano, *Principles of molecular photochemistry*, University Science Books, Sausalito, California, 2009.
10 I. Carmichael and G. L. Hug, *J. Phys. Chem. Ref. Data*, 1986, **15**, 1–250.
11 A. A. Gorman, I. Hamblett, C. Lambert, A. L. Prescott, M. A. J. Rodgers and H. M. Spence, *J. Am. Chem. Soc.*, 1987, **109**, 3091–3097.
12 J. F. Ireland and P. A. H. Wyatt, *J. Chem. Soc., Faraday Trans. 1*, 1973, **69**, 161–168.
13 A. Romani, F. Elisei, F. Masetti and G. Favaro, *J. Chem. Soc., Faraday Trans.*, 1992, **88**, 2147–2154.
14 L. Gu, H.-S. Chiang and A. Becker, *Int. J. Pharm.*, 1988, **41**, 95–104.
15 L. Gu, H.-S. Chiang and D. Johnson, *Int. J. Pharm.*, 1988, **41**, 105–113.
16 N. Ismail, L. Blancafort, M. Olivucci, B. Kohler and M. A. Robb, *J. Am. Chem. Soc.*, 2002, **124**, 6818–6819.
17 M. Merchan and L. Serrano-Andres, *J. Am. Chem. Soc.*, 2003, **125**, 8108–8109.

This journal is © The Royal Society of Chemistry 2013